PROFESSOR XIAODONG MA (Orcid ID : 0000-0002-5189-6287)

Article type : Research Article

Structural Optimization of Diphenylpyrimidine Scaffold as Potent and Selective Epidermal Growth Factor Receptor (EGFR) Inhibitors against L858R/T790M Resistance Mutation in Non-small Cell Lung Cancer

Yuanyuan Yi[a,1], Luhong Wang[c,1], Dan Zhao[c], Shanshan Huang[c], Changyuan Wang[c], Zhihao Liu [b,c], Huijun Sun[c], Kexin Liu[c], Xiaodong Ma[c,*] and Yanxia Li[a,*]

[a] *Department of Respiratory Medicine, the First Affiliated Hospital of Dalian Medical University, Dalian 116011, PR China*

[b] *State Key Laboratory of Bioactive Substance and Function of Natural Medicines, Institute of Materia Medica, Chinese Academy of Medical Sciences and Peking Union Medical College, Beijing 100050, P. R. China*

[c] *College of Pharmacy, Dalian Medical University, Dalian 116044, PR China*

[1] *These authors contributed equally to this work*

[*] *Corresponding author*

E-mail address: xiaodong.ma@139.com (X. Ma), liyanxia001@163.com (X. Li)

Abstract

A new class of thiodiphenylpyrimidine analogues (Thio-DPPY) were synthesized as potent and selective EGFR T790M inhibitors to overcome gefitinib resistance in non-small cell lung cancer (NSCLC). This structural optimization led to the identification of two potent $EGFR^{T790M/L858R}$ inhibitors, 1**4a** and **14e**, which possess IC_{50} values of 27.5 and 9.1 nM, respectively. Moreover, compounds **14a** (SI > 36.4) and **14e** (SI > 109.9) exhibited high selectivity and low activity against the wild type EGFR (IC_{50} > 1000 nM). In particular, compound **14a** also displayed strong potency against $EGFR^{T790M}$-mutated H1975 cells (IC_{50} = 0.074 μM), but weak activity toward normal cells HBE (IC_{50} > 40 μM) and LO-2 (IC_{50} = 9.891 μM). Importantly, compound **14a** (SI = 52.6) significantly improved the selectivity

against mutant H1975 cells over wild-type A431 cells than rociletinib (SI = 6.0), thus revealing its slight cell cytotoxicity. This study provides a promising Thio-DPPY derivative as enhanced EGFR T790M inhibitor, and also revealed valuable clues for further optimization of DPPY scaffold to overcome NSCLC resistance.

Keywords: NSCLC, EGFR T790M, Resistance, Inhibitors, Pyrimidine.

1. Introduction

The epidermal growth factor receptor (EGFR) tyrosine kinase is one of the most important clinically validated targets for non-small-cell lung cancer (NSCLC) treatment [1, 2]. First-generation EGFR inhibitors, gefitinib (**1**) and erlotinib (**2**), were approved by United States Food and Drug Administration (FDA) for treatment of NSCLC patients in 2003 and 2004, respectively (Fig.1) [3, 4]. Both of them achieved excellent improvements in overall response rates (ORR) and median progression-free survival (PFS) for NSCLC patients harboring with EGFR activating mutations (exon 19 deletion or exon 21 L858R substitution mutation) [5, 6]. Unfortunately, the secondary T790M (substitution of threonine to methionine) gatekeeper point mutation in exon 20, which accounts for approximately 60% of the drug resistances, often occurs for most NSCLC patients who are exhibiting activating mutations that are invariably developed acquired resistance to EGFR tyrosine kinase inhibitor (TKIs) therapy within months. The replacement of a threonine by the more sterically demanding methionine increases the affinity to ATP and provokes a steric repulsion of the 4-aminoquinazoline-based inhibitors erlotinib and gefitinib, resulting in a different binding mode and significant loss of inhibitory activity [7, 8].

Second-generation EGFR TKIs which incorporate a Michael acceptor to covalently target a rare cysteine (Cys797) in EGFR at the lip of the ATP-binding site were discovered to overcome EGFR T790M drug resistance. In these inhibitors, the electrophile represents the only distinctive feature as compared to first-generation EGFR inhibitors, and thus, the potential of these drugs to overcome T790M drug resistance is directly correlated with

covalent modification of the target protein [9, 10]. Afatinib (**3**) was the representative second-generation EGFR inhibitor, showing excellent clinical results to overcome EGFR T790M drug resistance. But for the dose limiting toxicities related to the inhibition of wild-type (WT) EGFR, the second EGFR inhibitor displayed limited clinical benefit for NSCLC patients who have developed T790M acquired resistance [11,12]. Therefore, third-generation covalent EGFR inhibitors, such as compounds **4** (WZ4002) [13], **5** (CO-1686, rociletinib) [14], and **6** (AZD9291, osimertinib) [15, 16], have been developed as mutant-selective EGFR inhibitors that specifically target EGFRL858R/T790M mutation while being less selective for WT EGFR (**Fig.1**). Generally, most of these third-generation EGFR T790M inhibitors feature a pyrimidine template along with an acrylamide functional substituent.

Sulfur, as the core chemical elements needed for biochemical functioning, is an elemental macronutrient for all life. A large number of sulphur-substituted organic molecules have been advanced to market for treatment of various disease, including Fudosteine (**7**) as a novel mucoactive agent [17], Omeprazole (**8**) as a medication used in the treatment of gastroesophageal reflux disease, peptic ulcer disease, and Zollinger–Ellison syndrome [18], Montelukast (**9**) as a leukotriene receptor antagonist (LTRA) used for the maintenance treatment of asthma and to relieve symptoms of seasonal allergies [19], and Modafinil (**10**) as a wakefulness-promoting agent (or eugeroic) used for treatment of disorders such as narcolepsy, shift work sleep disorder, and excessive daytime sleepiness associated with obstructive sleep apnea [20]. Notably, sulphor-submitted molecules also displayed excellent biological propriety for treatment of cancers. For example, Compound **11** is a typical JNK3 inhibitor [21], compound **12** is a EGFR inhibitor [22], and compound **13** is Bcl-2 inhibitor [23] (**Fig.2**). Based on the novel pyrimidine biological template [24], we synthesized a new class of thiopyrimidine derivatives to improve the activity and selectivity against EGFR T790M enzyme (**Fig.3**). Moreover, their activity against wild type EGFR and EGFR T790M-mutated enzymes, as well as their activity against NSCLC cell lines were also described in this manuscript.

2. Results and Discussion

2.1. Chemistry

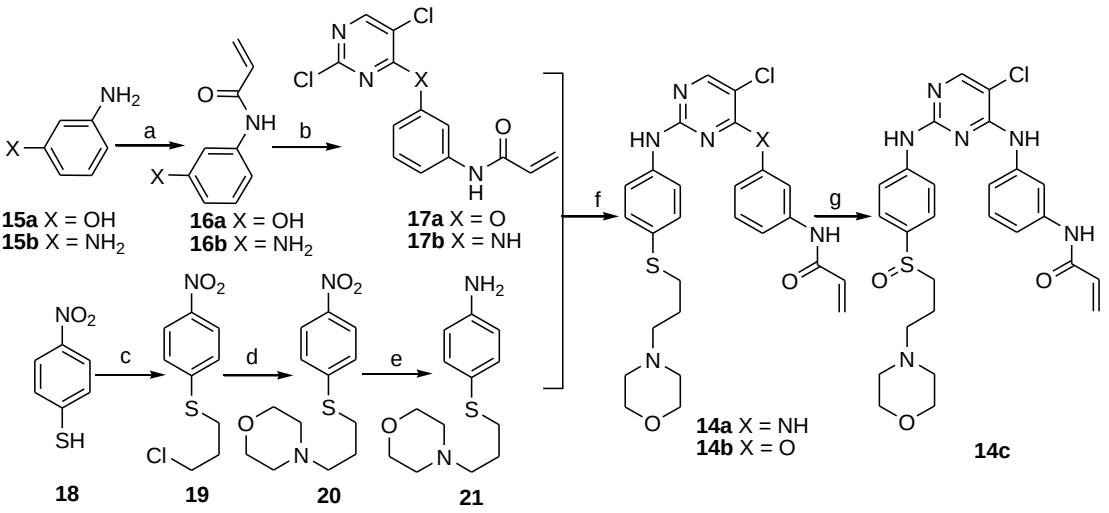

Scheme 1. Synthetic route of the title compounds **14a-c**. Reagents and conditions: (a) acryloyl chloride, $NaHCO_3$, CH_3CN, rt., 0.5 h, 60-80%; (b) X=OH, K_2CO_3, DMF, 60 °C; X=NH_2, DIPEA, 1,4-dioxane, rt., 2 h, 91%; (c) 1-chloro-3-bromopropane, K_2CO_3, CH_3CN, 70 °C, 12 h, 95%; (d) morpholine, K_2CO_3, KI, DMF, 80 °C, 12 h, 81%; (e) Fe-NH_4Cl, MeOH-H_2O, 2 h, 60 °C, 72%; (f) TFA, 2-BuOH, 100 °C, 12 h, 22-37%; (g) *m*-CPBA,CH_2Cl_2, rt., 31%.

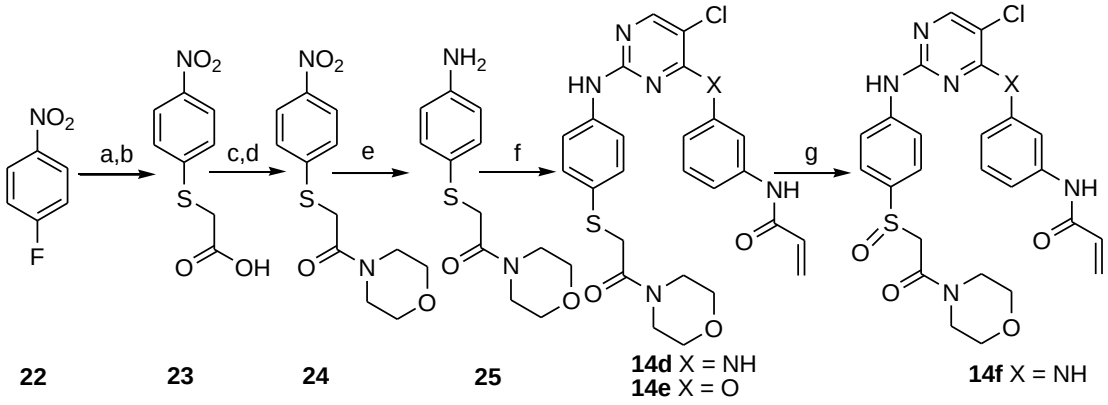

Scheme 2. Synthetic route of the title compounds **14d-f**. Reagents and conditions: (a) ethyl 2-mercaptoacetate, K_2CO_3, KI, DMF, 100 °C, 12 h, 95%; (b) KOH, H_2O, 50 °C, 24 h, 76%; (c) $SOCl_2$, 80 °C, 2 h; (d) morpholine, $NaHCO_3$, CH_3CN, rt, 0.5 h, 95%; (e) Fe-NH_4Cl, MeOH-H_2O, 2 h, 60 °C, 72%; (f) pyrimidines **17a-b**, TFA, 2-BuOH, 100 °C, 12 h, 16-19%, (g) *m*-CPBA,CH_2Cl_2, rt., 25%.

The synthetic routes of the title molecules **14a-f** are presented in Schemes 1 and 2 [25-28]. Commercially available anilines **15a**,**b** were reacted with acryloyl chloride to prepare the 3-acrylamide-substituted compounds **16a**,**b** in almost quantitative yields. By regioselectively coupling anilines **16a,b** with the 2,4,5-tricholrepyrimidine reagent, the key *C*-2 chloro-pyrimidine intermediates **17a,b** were synthesized. On the other hand, 4-nitrothiophenol **18** was reacted with 1-chloro-3-bromopropane to yield the chloro-substituted compound **19**, which was then converted to compound **20** characterized by a morpholine substituent. Next, the nitro-substituted compound **20** was reduced to the aniline derivative **21** by using the Fe-NH_4Cl condition. After completing the reaction between pyrimidines **17a,b** and aniline **21** under the action of trifluoroacetic acid (TFA), the title molecules **14a,b** were synthesized. Finally, oxidizing the sulfur atom in molecule **14a** with the *m*-chloroperbenzoic acid (*m*-CPBA) reagent prepared the sulfoxide-substituted compound **14c**. Similarly, the title molecules **14d-f** were also prepared as shown in Scheme 2. Starting from the reaction of 1-fluoro-4-nitrobenzene with ethyl 2-mercaptoacetate, the intermediate **23** was prepared, which was converted to nitro-substituted intermediate **24** *via* subsequent hydrolysis and acylation reactions. Compound **24** was then reduced to aniline **25** by using Fe-NH_4Cl reduction condition. By regionselectvie nucleophilic substitution and oxidation reactions, the desired molecules **14d-f** were conventionally synthesized.

2.2. Biological evaluation of 14a-f

2.2.1. Kinase inhibitory activity

Table 1 *In vitro* EGFR tyrosine kinases (wild type and L858R/T790M mutation) activities of the title compounds **14a-f** [a]

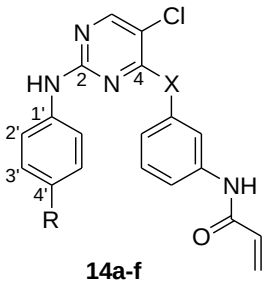

14a-f

Compound	X	R	Enzymatic activity (IC_{50}, nM)[b]		SI (WT: L858R/T790M)
			$EGFR^{L858R/T790M}$	$EGFR^{WT}$	
14a	NH	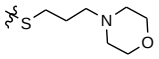	27.5±3.3	>1000	>36.4
14b	O	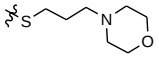	>100.0	1012±101.7	<10.1
14c	NH	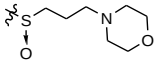	98.2±12.1	1035±81.5	10.4
14d	NH	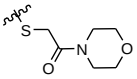	>100.0	980.0±72.4	<9.8
14e	O	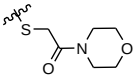	9.1±1.3	>1000	>109.9
14f	NH	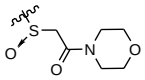	79.3±9.2	992.9±102.1	12.5
Rociletinib			20.0±4.3	500.0±67.5	25.0
Gefitinib			823.3±101.1	15.5±2.6	0.019

[a] Data represent the mean of at least three separate experiments.

[b] Concentration needed to inhibit the autophosphorylation of the cytoplasmic domain of EGFR by 50%, as calculated using software GraphPad Prim version 5.0.

The kinase-based activity against the wild type EGFR and the T790M/L858R-mutated EGFR was evaluated by using the ADP-Glo™ Kinase Assay system [29, 30]. Two novel EGFR inhibitors, gefitinib and rociletinib, were also tested as positive controls. The test results presented in table 1 clearly indicated that compounds **14a** and **14e** displayed the strongest anti-$EGFR^{T790M/L858R}$ activity among Thio-DPPYs, with IC_{50} values of of 27.5 and 9.1 nM, respectively. While the remaining compounds could effectviely inhibit $EGFR^{T790M/L858R}$ activity at concentrations of more than 79.3 nM. Structure and activity relationship analysis suggested that the oxidation of the sulfur atom to the sulfoxide group is unfavorable. For example, the sulfur-substituted analogue **14a** (IC_{50} = 27.5 nM) is markedly stronger than the analogue **14c** (IC_{50} = 98.2 nM) which bears a sulfoxide substituent. Fortunately, most of these compounds are inactive against the wild type EGFR (IC_{50} > 980 nM), indicating their high selectivity against the EGFR T790M mutation over the wild type EGFR. In particular, the potent inhibitors **14a** (SI > 36.4) and **14e** (SI > 110.2) possess greatly higher selectivity than rociletinib (SI = 25), which suggested that they will produce less side effects.

Table 2 Cellular antiproliferative activities of the title compounds **14a-f.**[a]

Compd.	Antiproliferative activity(IC_{50}, μM)[b]						SI (A431/ H1975)
	H1975	HCC827	A431	A549	LO2	HBE	
14a	0.074±0.011	0.152±0.088	3.893±0.708	5.794±1.022	9.891±1.236	>40	52.6
14b	0.373±0.091	0.204±0.091	5.762±1.089	5.842±0.931	16.50±2.090	38.5±3.1	15.4
14c	0.255±0.078	0.308±0.079	0.573±0.103	3.336±0.926	5.059±0.858	>40	2.2
14d	0.464±0.099	0.050±0.019	1.192±0.213	3.576±0.759	9.296±1.086	25.3±4.1	2.6
14e	1.050±0.125	0.198±0.087	7.557±0.834	8.493±2.010	20.90±3.147	>40	7.2
14f	0.667±0.101	0.062±0.011	2.247±0.947	33.97±5.78	14.77±2.014	>40	3.4
Rociletinib	0.299±0.092	0.031±0.009	1.794±0.965	3.242±0.945	12.75±2.084	>40	6.0
Gefitinib	4.691±1.050	0.006±0.001	3.300±0.817	10.07±1.03	21.86±4.152	23.8±3.2	0.7

[a] Data represent the mean of at least three separate experiments.

[b] Dose-response curves were determined at five concentrations. The IC_{50} values are the concentrations in micromolar needed to inhibit cell growth by 50% as determined from these curves.

2.2.2. Antiproliferative activity against NSCLC cell lines

In addition, all these compounds were evaluated for their activity against NSCLC cell lines using the MTT assay method. Four typical NSCLC cell lines (A431$^{\text{wild type EGFR}}$, H1975 $^{\text{EGFR T790M mutation}}$, A549 $^{\text{wild type EGFR and k-ras EGFR mutation}}$ and HCC827 $^{\text{EGFR del E746-A750 mutation}}$), and two normal cell lines (human bronchial epithelial cells(HBE), and liver cells(LO-2)) were used to evaluate the cell viability. As shown in Table 2, Thio-DPPY derivatives could actively interfere with the proliferation of gefitinib-resistant H1975 cells within the 0.074 (compound **14a**) to 1.050 μM (compound **14e**) concentrations range; however, they are less potent against the A431 cells harboring wild type EGFR ((compound **14c**, IC_{50} > 0.573 μM). In spite of the strong inhibitory potency toward the T790M-mutated EGFR enzyme, compound **14e** only displayed moderate capability for inhibiting the H1975 cells, with an IC_{50} value of 1.05 μM. Fortunately, compound **14a**, another potent $EGFR^{T790M}$ inhibitor,

exhibited strong potency against H1975 cells at a concentration of 0.074 μM. Compound **14a** also showed moderate activity to inhibit the proliferation of A431 cells (IC_{50} = 3.893 μM), indicating its high selectivity (SI = 52.6) toward mutant H1975 cells over wild type A431 cells. The activity against H1975 cells also showed that compounds **14d-f** (IC_{50} =0.464~1.05 μM) bearing a *N*-morpholine formamide functional group in the *C*-2 aniline side chain is slightly less active than the compounds **14a-c** (IC_{50} = 0.074~0.373 μM) without this substituent. Furthermore, all these compounds are highly sensitive to the HCC827 cell harboring EGFR del E746-A750 mutation, possessing IC_{50} values lower than 0.308 μM. Compound **14d**, the most active inhibitor against HCC827 cells in this series of compounds, particularly has an IC_{50} value of 0.050 μM. Additionally, all these compounds displayed moderate capability for inhibiting the A549 cells bearing the K-ras mutation. In terms of their activity against the normal cell lines HBE and LO-2, most of these Thio-DPPY derivatives are inactive**,** and the typical inhibitor **14a** (with IC_{50} values of 9.89 and 40 μM, respectively,) displayed considerably low cell cytotoxicity. **Figure 4** showed that the most active inhibitor **14a** significantly blocked the proliferation of H1975 cells with increasing time (24, 48, and 72 h) and drug concentrations (0.2, 0.5, and 1.0 μM). When treatment of 1.0 μM concentration of **14a** for 72 h, the cell viability rate (26.8%) was approximately 2-flod lower than that of rociletinib (44.8%), indicating enhanced anti-gefitinib resistance. These biological evaluations suggested that compound **14a** can be potentially used as a promising $EGFR^{T790M}$ inhibitor toward NSCLC.

2.2.3. Flow cytometry

The effect of the most potent inhibitor **14a** on the apoptosis in $EGFR^{T790M}$-mutated H1975 cells was also explored. As shown in **Figure 5**, compound **14a** could induce apoptosis in H1975 cells in a dose- and time-dependent manner. The apoptosis rates apparently increased from 45.6% to 96.8% in H1975 cells treated with compound **14a** (0.2, 0.5, and 1.0 μM) for 72 h.

2.3. Binding model analysis

To further elucidate the binding mode of the Thio-DPPY derivatives with the EGFR T790M enzyme, a docking study was performed using Autodock 4.2 software [31, 32]. The representative structures of **14a**, **14b**, **14c** and **14e** were docked into the crystal structure of the EGFR T790M binding pocket (PDB: 3IKA), respectively [13]. The autodock default parameters were used during the docking performance. For comparison, the lead compound WZ4002 was also docked into the binding pocket by using the same procedure. The simulation result showed in **Figure 6** indicated that compounds **14a** and **14b**, which possess strong inhibitory enzymatic activity, tightly bind with the EGFR T790M enzyme similarly to WZ4002. Typically, all these potent inhibitors formed several important contacts with $EGFR^{T790M}$ kinase, including (1) covalent-bond forces between the acrylamide group with the amino acid Cys797; (2) a strong contact generated from the chlorine atom at the *C*-5 position of the pyrimidine core with the mutant gatekeeper residue Met790; (3) strong hydrogen bonds between the *N*-1 nitrogen atom of the pyrimidine core and the amino acid Leu792. However, the less potent inhibitors **14b** and **14c** bind with $EGFR^{T790M}$ in a quite different manner from the active compounds, and almost lose these important interaction forces. These binding modes are accorded with their biological activity data.

3. Conclusion

To overcome gefitinib resistance in NSCLC, a class of Thio-DPPY derivatives were synthesized as potent and selective EGFR T790M inhibitors. Among these newly obtained compounds, two active $EGFR^{T790M}$ inhibitors **14a** and **14e** were identified, possessing IC_{50} values of 27.5 and 9.1 nM, respectively. Moreover, compounds **14a** (SI > 36.4) and **14e** (SI > 109.9) displayed less potency against the wild type EGFR (IC_{50} > 980 nM), but higher selectivity than rociletinib (SI = 25.0). In particular, compound **14a** exhibited strong potency against mutant H1975 cells (IC_{50} = 0.074 μM), and weak inhibitory ability toward the two normal cells HBE and LO-2 (with IC_{50} of 40 and 9.89 μM, respectively). All these results proved that inhibitor **14a** may be served as a potential EGFR T790M inhibitor to overcome gefitinib resistance toward NSCLC.

4. Experimental section

4.1. General Methods and Chemistry

All solvents and reagents were obtained from commercial supplies and were used without further purifications. Solvents were purified and stored according to standard procedures. High resolution ESI-MS was performed on an AB Sciex TripleTOF® 4600 LC/MS/MS system. ^{1}H NMR and ^{13}C NMR spectra on a Brucker AV 400 MHz spectrometer were recorded in [*d*] DMSO. Coupling constants (*J*) are expressed in hertz (Hz). Chemical shifts (δ scale) are reported in parts per million (ppm) relative to the central peak of the solvent. All reactions were monitored by TLC, using silica gel plates with fluorescence GF254 and UV light visualization. Flash chromatography separations were obtained on Silica Gel (300–400 mesh) using dichloromethane/methanol as eluents.

4.2. General procedure for the synthesis of the title compounds 14a,b and 14d,e.

2-Chloro-pyrimidine derivatives **17a,b** and the morpholine-substituted anilines intermediates **21**, **25** were synthesized according to our reported procedures [25-27]. All these intermediates were directly used without any purification and structural characterization. With these intermediates in hand, the title molecules **14a, b** and **14d, e** were synthesized as described below.

A flask was charged with intermediates **14a,b** (0.10 mmol), anilines **21, 25** (0.10 mmol), TFA (0.08 mL, 1.05 mmol), and 2-BuOH (10 mL). The slurry was heated to 100 °C for 12 h. The reaction mixture was allowed to cool to room temperature and was neutralized with a saturated aqueous sodium bicarbonate solution. The aqueous mixture was then extracted with CH_2Cl_2 (20 mL) three times. The crude product was purified using flash chromatography with dichloromethane/methanol (v/v, 30:1) as eluents.

4.2.1.N-[3-[[5-Chloro-2-[4-((1-morpholino)propylthio)phenylamino]-4-pyrimidinyl]amino] phenyl]-2-propenamide (14a)

Yield: 36.52%; off-yellow solid; ^{1}H NMR (400 MHz, DMSO-d_6): δ 1.60-1.63 (m, 2H), 2.28-2.32 (m, 6H), 2.82 (t, J = 8.0 Hz, 2H), 3.53 (t, J = 8.0 Hz, 4H), 5.76 (dd, J = 4.0 Hz, 8.0 Hz, 1H), 6.26 (dd, J = 4.0 Hz, 16.0 Hz, 1H), 6.44 (dd, J = 8.0 Hz, 16.0 Hz, 1H), 7.11 (d, J = 8.0 Hz, 2H), 7.18-7.35 (m, 2H), 7.52-7.57 (m, 3H), 7.89 (s, 1H), 8.15 (s, 1H), 9.00 (s, 1H), 9.41 (s, 1H), 10.22 (s, 1H); ^{13}C NMR (100 MHz, DMSO-d_6): δ 26.37, 32.42, 53.98 (2C), 57.39, 66.86 (2C), 104.60, 116.17, 116.24, 120.03 (2C), 120.14, 127.35, 127.64, 129.32, 131.03 (2C), 132.53, 139.46, 139.76, 139.83, 155.48, 156.96, 158.18, 163.84; HRMS (ESI) *m/z* calcd for $C_{26}H_{29}ClN_6O_4S$, $[M+H]^+$ 525.1834, found: 525.1843.

4.2.2.N-[3-[[5-Chloro-2-[4-((1-morpholino)propylthio)phenylamino]-4-pyrimidinyl]oxygen]phenyl]-2-propenamide (14b)

Yield: 22.14%; off-yellow solid; ^{1}H NMR (400 MHz, DMSO-d_6): δ 1.64-1.69 (m, 2H), 2.32-2.36 (m, 6H), 2.87 (t, J = 8.0 Hz, 2H), 3.58 (t, J = 8.0 Hz, 4H), 5.83 (dd, J = 4.0 Hz, 8.0 Hz, 1H), 6.32 (dd, J = 4.0 Hz, 16.0 Hz, 1H), 6.49 (dd, J = 12.0 Hz, 16.0 Hz, 1H), 7.06-7.10 (m, 3H), 7.40 (d, J = 8.0 Hz, 2H), 7.52 (d, J = 8.0 Hz, 2H), 7.76 (s, 1H), 8.54 (s, 1H), 9.89 (s, 1H), 10.46 (s, 1H); ^{13}C NMR (100 MHz, DMSO-d_6): δ 26.01, 31.83, 53.67 (2C), 57.04, 66.56 (2C), 105.09, 113.30, 117.02, 117.39, 119.75 (2C), 127.79, 128.01, 130.31 (2C), 130.39, 131.97, 138.56, 140.78, 152.66, 157.75, 158.51, 163.73, 164.26; HRMS (ESI) *m/z* calcd for $C_{26}H_{28}ClN_5O_3S$, $[M+H]^+$ 526.1674, found: 526.1678.

4.2.3.N-[3-[[5-Chloro-2-[4-((1-morpholino)ethanethioate)phenylamino]-4-pyrimidinyl]ami no]phenyl]-2-propenamide (14d)

Yield: 16.04%; off-white solid; ^{1}H NMR (400 MHz, DMSO-d_6): δ 3.41-3.54 (m, 8H), 3.80 (s, 2H), 5.76-5.79 (m, 1H), 6.28 (dd, J = 4.0 Hz, 16.0 Hz, 1H), 6.48 (dd, J = 8.0 Hz,16.0 Hz, 1H), 7.20 (d, J = 8.0 Hz, 2H), 7.36 (d, J = 8.0 Hz, 2H), 7.45-57 (m, 3H), 7.91 (s, 1H), 8.18 (s, 1H), 9.03 (s, 1H), 9.46 (s, 1H), 10.24 (s, 1H); ^{13}C NMR (100 MHz, DMSO-d_6): δ 37.70, 42.74, 47.14, 67.04 (2C), 105.06, 116.42, 116.59, 120.18 (2C), 120.48, 126.44, 127.95,

129.62, 132.30 (2C), 132.84, 139.75, 140.12, 140.71, 155.75, 157.25, 158.43, 164.15, 167.63; HRMS (ESI) *m/z* calcd for $C_{25}H_{25}ClN_6O_3S$, $[M+H]^+$ 525.1470, found: 525.1484.

4.2.4.N-[3-[[5-Chloro-2-[4-((1-morpholino)ethanethioate)phenylamino]-4-pyrimidinyl]oxygen]phenyl]-2-propenamide (14e)

Yield: 19.01%; off-white solid; ^{1}H NMR (400 MHz, DMSO-d_6): δ 3.39 (t, J = 4.0 Hz, 4H), 3.50 (t, J = 4.0 Hz, 4H), 3.77 (s, 2H), 5.77 (dd, J = 4.0 Hz, 8.0 Hz, 1H), 6.26 (dd, J = 4.0 Hz, 16.0 Hz, 1H), 6.45 (dd, J = 8.0 Hz, 16.0 Hz, 1H), 7.00-7.03 (m, 1H), 7.11 (d, J = 8.0 Hz, 2H), 7.35 (d, J = 8.0 Hz, 2H), 7.46 (d, J = 8.0 Hz, 1H), 7.57 (d, J = 8.0 Hz, 1H), 7.70 (s, 1H), 8.48 (s, 1H), 9.85 (s, 1H), 10.39 (s, 1H); ^{13}C NMR (100 MHz, DMSO-d_6): δ 36.89, 42.14, 46.51, 66.43 (2C), 105.30, 113.26, 117.09, 117.43, 119.60 (2C), 126.84, 127.81, 130.40, 131.36 (2C), 131.98, 139.24, 140.78, 152.67, 157.74, 158.50, 163.77, 164.28, 166.95; HRMS (ESI) *m/z* calcd for $C_{25}H_{24}ClN_5O_4S$, $[M+H]^+$ 526.1310, found: 526.1323.

4.3. General procedure for the synthesis of the title compounds 14c,f.

m-CPBA (75%) (0.24 g, 1.03 mmol) was added to a solution of **14a** or **14d** (0.25 g, 0.52 mmol) in anhydrous CH_2Cl_2 (10 mL) at 0 °C. The reaction mixture was allowed to warm to room temperature and then stirred for 1 h. The solution was diluted with CH_2Cl_2 and then treated with 50% $Na_2S_2O_3$/$NaHCO_3$ solution. The organic layer was separated, washed with brine, dried with Na_2SO_4, filtered, and concentrated in vacuo. The resulting crude material was subjected to flash column chromatography (CH_2Cl_2/MeOH stepwise elution, 30:1) to give the title molecules **14c,f** .

4.3.1.N-[3-[[5-Chloro-2-[4-((1-morpholino)propylsulfinyl)phenylamino]-4-pyrimidinyl]amino]phenyl]-2-propenamide (14c)

Yield: 31.0%; off-brown solid; ^{1}H NMR (400 MHz, DMSO-d_6): δ 1.56-1.68 (m, 2H), 2.26-2.32 (m, 6H), 2.74-2.86 (m, 2H), 3.52 (t, J = 8.0 Hz, 4H), 5.76 (dd, J = 4.0 Hz, 8.0 Hz, 1H), 6.27 (dd, J = 4.0 Hz, 16.0 Hz, 1H), 6.48 (dd, J = 12.0 Hz, 16.0 Hz, 1H), 7.30-7.40 (m, 5H), 7.53-7.58 (m, 1H), 7.83 (d, J = 8.0 Hz, 2H), 8.22 (s, 1H), 9.10 (s, 1H), 9.73 (s, 1H),

10.28 (s, 1H); ^{13}C NMR (100 MHz, DMSO-d_6): δ 19.14, 19.47, 53.68 (2C), 57.13, 66.78 (2C), 105.28, 114.31, 116.17, 116.35, 119.33 (2C), 125.25 (2C), 126.64, 127.63, 129.53, 132.56, 135.60, 139.91, 143.62, 155.47, 157.03, 158.01, 163.86; HRMS (ESI) *m/z* calcd for $C_{26}H_{29}ClN_6O_3S$, $[M+H]^+$ 541.1783, found: 541.1788.

4.3.2.N-[3-[[5-Chloro-2-[4-((1-morpholino)acetylsulfinyl)phenylamino]-4-pyrimidinyl]amino]phenyl]-2-propenamide (14f)

Yield: 25.0%; off-brown solid; ^{1}H NMR (400 MHz, DMSO-d_6): δ 3.37-3.52 (m, 8H), 3.93 (d, J = 12.0 Hz, 1H), 4.11 (d, J = 12.0 Hz, 1H), 5.77 (dd, J = 4.0 Hz, 8.0 Hz, 1H), 6.27 (dd, J = 4.0 Hz, 16.0 Hz, 1H), 6.47 (dd, J = 8.0 Hz,16.0 Hz, 1H), 7.37 (d, J = 8.0 Hz, 2H), 7.49 (d, J = 8.0 Hz, 2H), 7.82-7.94 (m, 4H), 8.22 (s, 1H), 9.11 (s, 1H), 9.72 (s, 1H), 10.25 (s, 1H); 13C NMR (100 MHz, DMSO-d_6): δ 42.39, 46.71, 61.09, 66.61, 66.78, 105.36, 116.23, 116.43, 119.23 (2C), 120.43, 125.78 (2C), 127.71, 129.36, 132.53, 135.41, 139.40, 139.91, 143.96, 155.48, 157.09, 158.01, 163.89, 163.91; HRMS (ESI) *m/z* calcd for $C_{25}H_{25}ClN_6O_4S$, $[M+H]^+$] 541.1419, found: 541.1441.

4.4. Kinase enzymatic assays

ADP-Glo^{TM} assay systems (EGFR^{WT}: Catalog. V3831, EGFR$^{T790M/L858R}$: Catalog. V5324), were purchased from Promega Corporation (USA). The experiments were performed according to the instructions of the manufacturer. The detailed and complete protocols, and the active kinase data were available at: https://cn.promega.com/resources/protocols/product-information-sheets/n/egfr-kinase-enzyme-system-protocol/ and https://cn.promega.com/resources/protocols/product-information-sheets/n/egfr-t790m-l858r-kinase-assay-protocol/, respectively. For all of the tested compunds, concentrations consisting of suitable levels from 0.1 to 1000 nM were used. The test was performed in a 384-well plate, including the main steps below: (1) perform a 5 μL kinase reaction using 1× kinase buffer (e.g., 1× reaction buffer A), (2) incubate at room temperature for 60 minutes, (3) add 5 μL of ADP-Glo™ reagent to stop the kinase reaction and deplete theunconsumed ATP, leaving

only ADP and a very low background of ATP, (4) incubate at room temperature for 40 minutes, (5) add 10 μL of kinase detection, (6) reagent to convert ADP to ATP andintroduce luciferase and luciferin to detect ATP, (7) incubate at room temperature for 30 minutes, (8) plate was measured on TriStar® LB942 Multimode Microplate Reader (BERTHOLD) to detect the luminescence (Integration time 0.5-1 second). Curve fitting and data presentations were performed using GraphPad Prism version 5.0.

4.5. Cellular activity assay

H1975, H431, HCC827, and A549 human NSCLC cells were obtained from the American Type Culture Collection. HBE cells and LO-2 cells were kind gifts from Fuheng Biology Company (Shanghai, China). H1975, HCC827 and A549 cells were grown in RPMI-1640 (Gibco®, USA) supplemented with 10% FBS (Gibco®, USA), 1% penicillin-streptomycin (Beyotime Company, China). A431 , LO-2 and HBE cells were grown in DMEM (Gibco®, USA) supplemented with 10% FBS (Gibco®, USA), 1% penicillin-streptomycin (Beyotime Company, China). All cells were maintained and propagated as monolayer cultures at 37 °C in humidified 5% CO_2 incubator.

Cell viability was then assessed with MTT reagent (Thiazolyl blue tetrazolium bromide; Sigma, Oakville, ON). Cells were seeded in 96-well plates at a density of 3,000 to 5,000 cells/well and were maintained at 37 °C in a 5% CO_2 incubator in DMEM or RPMI1640 containing 10% fetalbovine serum (FBS, Gibco®). Cells were esposed to treatment for 72 h, and the number of cells used per experiment for each cell lines was adjusted to obtain an absorbance of 0.5 to 1.2 at 570 nm. Compounds were tested at appropriate concentrations (0.01 to 40 μM), with each concentration duplicated five times. The data were calculated using GraphPad Prim version 5.0. Dose-response curves were fitted using a nonlinear regression model with a sigmoidal dose-response.

4.6. Molecular docking study

AutoDock 4.2 software and the default parameter was used to perform the docking studies. Detailed tutorials that guide users through basic AutoDock usage, docking with flexible rings, and virtual screening with AutoDock may be found at: http://autodock.scripps.edu/faqs-help/tutorial. Generally, the crystal structure (PDB: 3IKA) of the kinase domain of $EGFR^{T790M}$ bound to inhibitor **4** was used in the docking studies. The enzyme preparation and the hydrogen atoms adding was performed in the prepared process. The whole EGFR enzyme was defined as a receptor and the site sphere was selected on the basis of the binding location of WZ4002. By moving WZ4002 and the irrelevant water, molecules **14a**, **b, c** and **e** were placed, respectively. When doing the molecular simulation, the covalent bond produced by the acryloyl group and the amino acid Cys797 is set as default if the distance between them is low than 3.82 Å (Within this distance, WZ4002 could form covalent bond with Cys797). The binding interaction energy was calculated to include Van der Waals, electrostatic, and torsional energy terms defined in the tripos force field. The structure optimization was performed using a genetic algorithm, and only the best-scoring ligand protein complexes were kept for analyses.

Acknowledgements

We are grateful to the National Natural Science Foundation of China (No. 81672945, 81603186), and Research Fund of Higher Education of liaoning province（LQ2017039）for the financial support of this research.

Figure legends

Figure 1. Novel EGFR inhibitors for treatment of NSCLC.

Figure 2. Chemical structures of the typical organosulfur compounds.

Figure 3. Designed strategy of the Thio-DPPY derivatives.

Figure 4. The effects of treating time and drug concentrations of compound 14a and rociletinib on H1975 cell viability, (A) inhibitor **14a**; (B) rociletinib.

Figure 5. Compound **14a** induced H1975 cell apoptosis *in vitro*. The cells were incubated with the indicated concentrations of **14a** for 72 h, and the cells were stained with annexinV/FTIC, followed by flow cytometry analysis. One representative experiment is shown.

Figure 6. A: Binding mode of WZ4002 with $EGFR^{T790M}$ enzyme (PDB code: 3IKA); B,C,D,E: Proposed binding modes of the typical inhibitors with $EGFR^{T790M}$ enzyme (B: inhibitor **14a**, C: inhibitor **14e**, D: inhibitor **14b**, E: inhibitor **14c**).

Conflict of interest

All these authors were employed by Dalian Medical University, and all of them have no financial and personal relationships with other people or organizations that can inappropriately influence this work.

References

[1] S.M. Huang, P.M. Harari, Epidermal growth factor receptor inhibition in cancer therapy: biology, rationale and preliminary clinical results, Invest. New Drug 17 (1999) 259−269.

[2] C.E. Steuer, F.R. Khuri, S.S. Ramalingam, The next generation of epidermal growth factor receptor tyrosine kinase inhibitors in the treatment of lung cancer, Cancer 121 (2015) E1−E6.

[3] M.H. Cohen, G.A. Williams, R. Sridhara, G. Chen, W.D. McGuinn, D. Morse, S. Abraham, A. Rahman, C. Liang, R. Lostritto, A. Baird, R. Pazdur, United states food and drug administration drug approval summary: gtefitinib (ZD1839; Iressa) tablets, Clin. Cancer Res. 10 (2004) 1212−1218.

[4] M.H. Cohen, J.R. Johnson, Y.F. Chen, R. Sridhara, R. Pazdur, FDA drug approval summary: erlotinib (tarceva) tablets, Oncologist 10 (2005) 461−466.

[5] F.R. Hirsch, P.A. Janne, W.E. Eberhardt, F. Cappuzzo, N. Thatcher, R. Pirker, H. Choy, E.S. Kim, L. Paz-Ares, D.R. Gandara, Y.L. Wu, M.J. Ahn , T. Mitsudomi, F.A. Shepherd, T.S. Mok, Epidermal growth factor receptor inhibition in lung cancer: status 2012, J. Thorac. Oncol. 8 (2013) 373−384.

[6] S.H. Lim, J.Y. Lee, J.M. Sun, J.S. Ahn, K. Park, M.J. Ahn, Comparison of clinical outcomes following gefitinib and erlotinib treatment in non-small-cell lung cancer patients harboring an epidermal growth factor receptor mutation in either exon 19 or 21, J. Thorac. Oncol. 9 (2014) 506−511.

[7] C.H. Yun, K.E. Mengwasser, A.V. Toms, M.S. Woo, H. Greulich, K.K. Wong, M. Meyerson, M.J. Eck, The T790M mutation in EGFR kinase causes drug resistance by increasing the affinity for ATP, P. Natl. Acad. Sci. USA 105 (2008) 2070−2075.

[8] S. Ghosh, Y. Zheng, X. Jun, R.K. Narla, S. Mahajan, C. Navara, C. Mao, E.A. Sudbeck, F.M. Uckun, Alpha-cyano-beta-hydroxy-beta-methyl-*N*-[4-(trifluoromethoxy)phenyl] propenamide: an inhibitor of the epidermal growth factor receptor tyrosine kinase with potent cytotoxic activity against breast cancer cells, Clin. Cancer Res. 4 (1998) 2657−2668.

[9] L. Tan, J. Wang, J. Tanizaki, Z. Huang, A.R. Aref, M. Rusan, S.J. Zhu, Y. Zhang, D. Ercan, R.G. Liao, M. Capelletti, W. Zhou, W. Hur, N. Kimn, T. Sim, S. Gaudet, D.A. Barbie, J.R.J. Yeh, C.H. Yun, P.S. Hammerman, M. Mohammadi, P.A. Janne, N.S. Gray, Development of covalent inhibitors that can overcome resistance to first-generation FGFR kinase inhibitors, P. Natl. Acad. Sci. USA 111 (2015) E4869−E4877.

[10] J.R. Gomes, M.R.S. Cruz, Combination of afatinib with cetuximab in patients with EGFR-mutant non-small-cell lung cancer resistant to EGFR inhibitors, Oncotargets Ther. 8 (2015) 1137−1142.

[11] C. Rolfo, E. Giovannetti, D.S. Hong, T. Bivona, L.E. Raez, G. Bronte, L. Buffoni, N. Reguart, E.S. Santos, P. Germonpre, M. Taron, F. Passiglia, J.P. Van, A. Russo, M. Peeters, I. Gil-Bazo, P. Pauwels, R. Rosell, Novel therapeutic strategies for patients with NSCLC that do not respond to treatment with EGFR inhibitors, Cancer Treatment Rev. 40 (2014) 990−1004.

[12] H.J. Lee, G. Schaefer, T. Heffron, S. Malek, M. Merchant, R.L. Yauch, V. Pirazzoli, K. Politi, J. Settleman, Abstract LB-309: Non-covalent wild-type-sparing inhibitors of EGFR T790M, Cancer Res. 73 (2013) LB309−LB309.

[13] W. Zhou, D. Ercan, L. Chen, C.H. Yun, D. Li, M. Capelletti, A.B. Cortot, L. Chirieac, R.E. Iacob, R. Padera, J.R. Engen, K.K. Wong, M.J. Eck, N.S. Gray, P.A. Janne, Novel

mutant-selective EGFR kinase inhibitors against EGFR T790M, Nature 462 (2009) 1070−1074.

[14] A.O. Walter, R.T. Sjin, H.J. Haringsma, K. Ohashi, J. Sun, K. Lee, A. Dubrovskiy, M. Labenski, Z. Zhu, Z. Wang, M. Sheets, T.S. Martin, R. Karp, D. Kalken, P. Chaturvedi, D. Niu, M. Nacht, R.C. Petter, W. Westlin, K. Lin, S. Jaw-Tsai, M. Raponi, T.V. Dyke, J. Etter, Z. Weaver, W. Pao, J. Singh, A.D. Simmons, T.C. Harding, A. Allen, Discovery of a mutant-selective covalent inhibitor of EGFR that overcomes T790M-mediated resistance in NSCLC, Cancer Discov. 3 (2013) 1404−1415.

[15] D.A. Cross, S.E. Ashton, S. Ghiorghiu, C. Eberlein, C.A. Nebhan, P.J. Spitzler, J.P. Orme, M.R. Finlay, R.A. Ward, M.J. Mellor, G. Hughes, A. Rahi, V.N. Jacobs, M.R. Brewer, E. Ichihara, J. Sun, H. Jin, P. Ballard, K. Al-Kadhimi, R. Rowlinson, T. Klinowska, G.H. Richmond, M. Cantarini, D.W. Kim, M.R. Ranson, W. Pao, AZD9291, an irreversible EGFR TKI, overcomes T790M-mediated resistance to EGFR inhibitors in lung cancer, Cancer Discov. 4 (2014) 1046−1061.

[16] M.R. Finlay, M. Anderton, S. Ashton, P. Ballard, P.A. Bethel, M.R. Box, R.H. Bradbury, S.J. Brown, S. Butterworth, A. Campbell, C. Chorley, N. Colclough, D.A. Cross, G.S. Currie, M. Grist, L. Hassall, G.B. Hill, D. James, M. James, P. Kemmitt, T. Klinowska, G. Lamont, S.G. Lamont, N. Martin, H.L. McFarland, M.J. Mellor, J.P. Orme, D. Perkins, P. Perkins, G. Richmond, P. Smith, R.A. Ward, M.J. Waring, D. Whittaker, S. Wells, G.L. Wrigley, Discovery of a potent and selective EGFR inhibitor (AZD9291) of both sensitizing and T790M resistance mutations that spares the wild type form of the receptor, J. Med. Chem. 57 (2014) 8249−8267.

[17] G.O. Osoata, T. Hanazawa, C. Brindicci, M. Ito, P.J. Barnes, S. Kharitonov, K. Ito, Peroxynitrite elevation in exhaled breath condensate of COPD and its inhibition by fudosteine, Chest. 135 (2009) 1513−1520.

[18] N. Dzeletovic, J. McGuire, M. Daujat, J. Tholander, M. Ema, Y. Fujii-Kuriyama, J. Bergman, P. Maurel, L. Poellinger, Regulation of dioxin receptor function by omeprazole, J. Biol. Chem. 272 (1997) 12705−12713.

[19] A. Markham, D. Faulds, Montelukast, Drugs 56 (1998) 251−256.

[20] J.W. Young, M.A. Geyer, Action of modafinil--increased motivation via the dopamine transporter inhibition and D1 receptors? Biol. Psychiatry. 67 (2010) 784−787.

[21] F. Muth, A. El-Gokha, F. Ansideri, M. Eitel, E. Doring, A. Sievers-Engler, A. Lange, F.M. Boeckler, M. Lammerhofer, P. Koch, S.A. Laufer, Tri- and tetra-substituted pyridinylimidazoles as covalent inhibitors of *c*-Jun *N*-terminal kinase 3, J. Med. Chem. 60 (2016) 594−607.

[22] V. Chandregowda, A.K. Kush, R.G. Chandrasekara, Synthesis and in vitro antitumor activities of novel 4-anilinoquinazoline derivatives, Eur. J. Med. Chem. 44 (2009) 3046−3055.

[23] C. Tse, A.R. Shoemaker, J. Adickes, M.G. Anderson, J. Chen, S. Jin, E.F. Johnson, K.C. Marsh, M.J. Mitten, P. Nimmer, L. Roberts, S.K. Tahir, Y. Xiao, X. Yang, H. Zhang, S. Fesik, S.H. Rosenberg, S.W. Elmore, ABT-263: a potent and orally bioavailable Bcl-2 family inhibitor, Cancer Res. 68 (2008) 3421−3428.

[24] Z. Song, Y. Ge, C. Wang, S. Huang, X. Shu, K. Liu, Y. Zhou, X. Ma, Challenges and perspectives on the development of small-molecule EGFR inhibitors against T790M-mediated resistance in non-small-cell lung cancer, J. Med. Chem. 59 (2016) 6580−6594.

[25] A. Song, J. Zhang , Y. Ge, C. Wang, Q. Meng, Z. Tang, J. Peng, K. Liu, Y. Li, X. Ma, *C*-2 (*E*)-4-(Styryl)aniline substituted diphenylpyrimidine derivatives (Sty-DPPYs) as specific kinase inhibitors targeting clinical resistance related EGFRT790M mutant, Bioorg. Med. Chem. 25 (2017) 2724–2729.

[26] H. Liu, B. Wu, Y. Ge, J. Huang, S. Song, C. Wang, J. Yao, K. Liu, Y. Li, Y. Li, X. Ma, Phosphamide-containing diphenylpyrimidine analogues (PA-DPPYs) as potent focal adhesion kinase (FAK) inhibitors with enhanced activity against pancreatic cancer cell lines. Bioorg. Med. Chem. 25 (2017) 6313–6321.

[27] Z. Song, Y. Jin, Y. Ge, C. Wang, J. Zhang, Z. Tang, J. Peng, K. Liu, Y. Li, X. Ma, Synthesis and biological evaluation of azole-diphenylpyrimidine derivatives (AzDPPYs) as potent T790M mutant form of epidermal growth factor receptor inhibitors, Bioorg. Med. Chem. 24 (2016) 5505−5512.

[28] S. Chang, L. Zhang, S. Xu, J. Luo, X. Lu, Z. Zhang, T. Xu, Y. Liu, Z. Tu, Y. Xu, X. Ren, M. Geng, J. Ding, D. Pei, K. Ding, Design, synthesis, and biological evaluation of novel conformationally constrained inhibitors targeting epidermal growth factor receptor threonine790→methionine790 mutant, J. Med. Chem. 55 (2012) 2711−2723.

[29] H. Zegzouti, M. Zdanovskaia, K. Hsiao, S.A. Goueli, ADP-Glo: A Bioluminescent and homogeneous ADP monitoring assay for kinases, Assay Drug Dev. Technol. 7 (2009) 560−572.

[30] B. Heedmann, M. Klumpp, Screening for inhibitors of kinase autophosphorylation, Methods Mol. Biol. 1439 (2016) 159−169.

[31] G.M. Morris, R. Huey, W. Lindstrom, M.F. Sanner, R.K. Belew, D.S. Goodsell, A.J. Olson, AutoDock4 and AutoDockTools4: automated docking with selective receptor flexibility, J. Comput. Chem. 30 (2009) 2785−2791.

[32] A.E. Lohning, S.M. Levonis, B. Williams-Noonan, S.S. Schweiker, A practical guide to molecular docking and homology modelling for medicinal chemists, Curr. Top. Med. Chem. 17 (2017) 2023−2040.

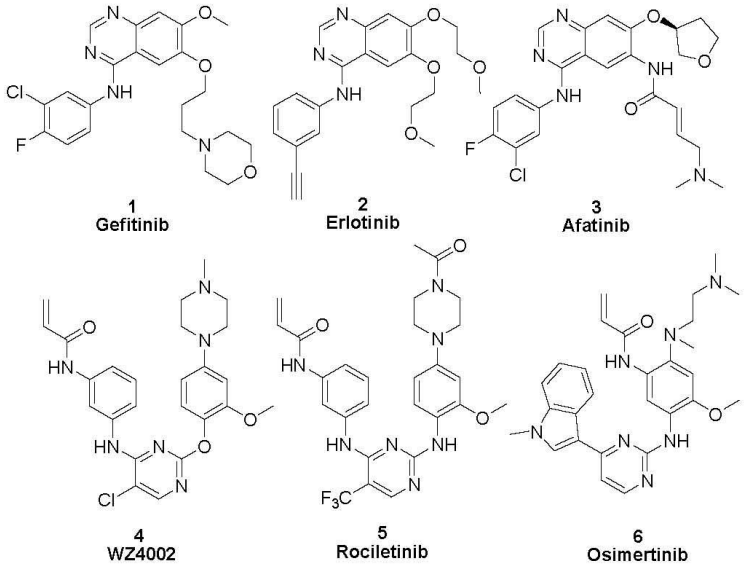

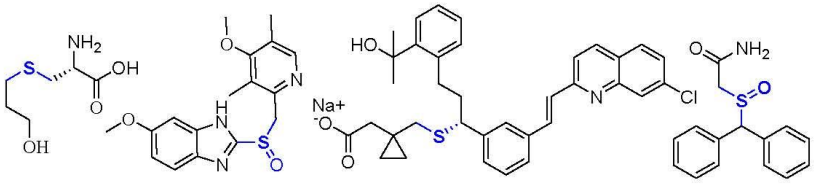

7 Fudosteine **8** Omeprazole **9** Montelukast sodium **10** Modafinil

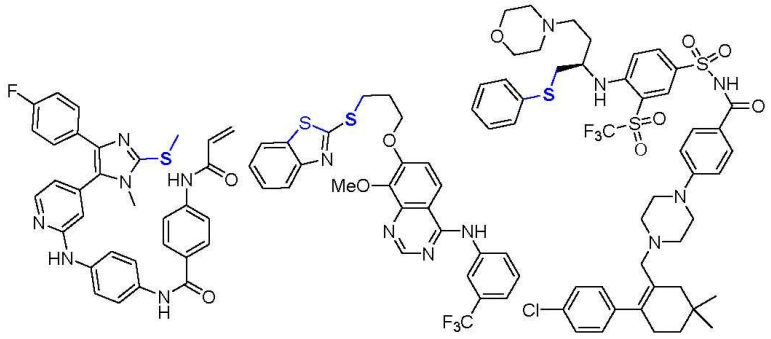

11 JNK3 Inhibitor
IC_{50} (JNK3) = 0.3 nM

12 EGFR Inhibitor
IC_{50} (A431) = 4.50 μM
IC_{50} (MCF-7) = 35.90 μM

13 Navitoclax
Bcl-2 inhibitor
IC_{50} (Bcl-2) ≤ 1 nM
phase Ⅱ